Available online at www.sciencedirect.com
ScienceDirect
Journal of the European Ceramic Society 27 (2007) 2855–2859
www.elsevier.com/locate/jeurceramsoc

Effect of Al_2O_3 on the structure and microwave dielectric properties of $Ca_{0.7}Ti_{0.7}La_{0.3}Al_{0.3}O_3$

G.A. Ravi, F. Azough *, R. Freer

Manchester Materials Science Centre, School of Materials, University of Manchester, Grosvenor Street, Manchester M1 7HS, UK

Available online 18 December 2006

Abstract

The effect of excess Al_2O_3 on the densification, structure and microwave dielectric properties of $Ca_{0.7}Ti_{0.7}La_{0.3}Al_{0.3}O_3$ (CTLA) was investigated. CTLA ceramics were prepared using the conventional mixed oxide route. Excess Al_2O_3 in the range of 0.1–0.5 wt% was added. It was found that Al_2O_3 improved the densification. A phase rich in Ca and Al was found in the microstructure of Al_2O_3 doped samples. Additions of Al_2O_3 coupled with the slow cooling after sintering improved the microwave dielectric properties. CTLA ceramics with 0.25 wt% Al_2O_3 cooled at 5 °C/h showed high density and a uniform grain structure with $\varepsilon_r = 46$, $Q \times f = 38{,}289$ and $\tau_f = +12$ ppm/°C at 4 GHz. XRD and TEM examinations showed the presence of (1 1 2) and (1 1 0) type twins arising from $a^-a^-c^+$ tilt system with the presence of anti-phase domain boundaries from the displacement of A-site cations of the orthorhombic perovskite structure.

Keyword: Microwave dielectrics

1. Introduction

Materials with the perovskite structure are widely employed as dielectric resonators, because of their high dielectric constants and high quality factors. Perovskites are characterised by the chemical formula ABO_3, and a structure which is very tolerant to substitution of ions of various sizes on both A and B cation sublattices.[1] At room temperature many of these perovskites compounds are distorted from the ideal structure through rotation or tilting of the BO_6 octahedra accompanied by displacement of the A-site cations. As a result, most of the perovskites at room temperature exhibit sub-grain features. Such as twining domains and ordering anti-phase boundaries due to the structural phase transitions, which are encountered during cooling from the sintering temperature.[2–4]

$CaTiO_3$ is an orthorhombic distorted perovskite[5] at room temperature with high relative permittivity ($\varepsilon_r = 170$), modest quality factor ($Q \times f = 3500$ GHz) and a very high positive temperature coefficient of resonant frequency ($\tau_f = +800$ ppm/°C).[4,6] In contrast $LaAlO_3$ is a rhombohedral perovskite at room temperature[7] with low relative permittivity ($\varepsilon_r = 23.4$), high quality factor ($Q \times f = 68{,}000$ GHz) and a negative temperature coefficient of resonant frequency ($\tau_f = -44$ ppm/°C).[7] The high positive τ_f of $CaTiO_3$ can be suppressed to small or zero τ_f by addition of $LaAlO_3$, which make it a suitable candidate for microwave applications. Ceramic material based on $CaTiO_3$–$LaAlO_3$ solid solution[8] is a promising candidate for microwave frequencies because of its high dielectric constant ($\varepsilon_r \approx 45$–47) with high quality factor ($Q \times f \approx 38{,}000$) and small or zero temperature coefficient of resonant frequency (τ_f).

Suvorov et al.[6] reported dielectric properties of $\varepsilon_r = 44$, $Q \times f = 30{,}000$ and $\tau_f = -3$ ppm/°C for $0.7CaTiO_3$–$0.3LaAlO_3$. High calcination temperature in the range of 1350–1450 °C for 40 h with intermediate grinding was reported. The sintering temperature was 1450 °C for 12 h. They reported the existence of a significant amount of closed porosity. The densification of the CTLA ceramic was improved by increasing the LA ($LaAlO_3$) content or substitution of 1 at% Sr for Ca. Moon et al.[9] also studied the dielectric and sintering properties of $(1-x)CaTiO_3$–$xLaAlO_3$ ceramics. A high calcinations temperature of 1400 °C and high sintering temperature of 1600 °C were required to obtain dense ceramics. Additions of combinations of Bi_2O_3 with Al_2O_3 or NiO lowered the sintering temperature to 1450 °C. However, the additives reduced the $Q \times f$ value by at least 15%. The microwave dielectric properties of $\varepsilon_r \approx 45$, $Q \times f \approx 22{,}500$ GHz and $\tau_f \approx +10$ ppm/°C were reported for the undoped $0.7CaTiO_3$–$0.3LaAlO_3$.[9]

* Corresponding author. Tel.: +44 161 7796300x412; fax: +44 161 3068840.
E-mail address: feridoon.azough@manchester.ac.uk (F. Azough).

0955-2219/$ – see front matter © 2006 Elsevier Ltd. All rights reserved.
doi:10.1016/j.jeurceramsoc.2006.11.010

In the present study, the effect of excess Al_2O_3 and the change of cooling rate on the sintering behaviour, microstructure and microwave dielectric properties of $0.7CaTiO_3$–$0.3LaAlO_3$ ceramics have been investigated.

2. Experimental

Samples were prepared by conventional mixed oxide route. High purity (>99.9%) $CaCO_3$, TiO_2, La_2O_3 and Al_2O_3 were used as raw materials. The powders were weighed according to the stoichiometry ($Ca_{0.7}Ti_{0.7}La_{0.3}Al_{0.3}O_3$) and mixed for 20 h using propan-2-ol and zirconia media. La_2O_3 was dried at 900 °C for 6 h before weighing. The mixed powders were calcined at 1250 °C for 4 h then 0.25 wt% Al_2O_3 was added and wet milled for 20 h and dried. Pellets were prepared by pressing powders in steel die 20 mm diameter at 100 MPa. The pellets were sintered at 1500 °C for 4 h in air with a heating rate of 180 °C/h and cooling rate of 180 °C/h. Selected samples were also cooled at 60, 15 and 5 °C/h.

Crystal structures were examined by X-ray diffraction (Philips Analytical, X'pert-MPD) employing Cu Kα1 radiation under the conditions 50 kV and 40 mA. The samples were scanned at 0.03° intervals of 2θ in the range 10–85°; the scan rate was $0.01° \, 2\theta \, s^{-1}$.

Microstructural examination of the sintered ceramics was performed by means of scanning electron microscopy (SEM) (JEOL 6300 and PHILIPS XL30). The sintered surfaces of ceramics were ground (to 1200 grade SiC) and polished (to 1 μm diamond paste). Then, samples were thermally etched at 1320° for 12 min and coated with carbon prior to SEM analysis.

TEM specimens were prepared from the sintered ceramics, after lapping and polishing to form 3 mm diameter discs. The discs were dimpled to reduce the sample to 30 μm thickness in the centre and then thinned to electron transparency with a Gatan Precision Ion Polishing System (PIPS). The specimens were investigated using a Philips CM200 operating at 200 kV and a Tecnai G2 TEM operating at 300 kV. The dielectric properties (ε_r and $Q \times f$) were determined by the parallel plate method.[10] The τ_f values were determined using a silver-plated, aluminium cavity at temperatures between −10 and +60 °C.

3. Results and discussion

3.1. Densification

The density of undoped $Ca_{0.7}Ti_{0.7}La_{0.3}Al_{0.3}O_3$ sample was only 90% theoretical after sintering at 1500 °C for 4 h. Addition of 0.15 wt% Al_2O_3 improved the densification to 93%, whereas 0.25 wt% Al_2O_3 increased density to 96%. Addition of alumina in excess of 0.25–0.3 and 0.5 wt% decreased density to 92 and 90%, respectively. Addition of the excess alumina did not affect the sintering temperature or sintering time.

3.2. X-ray diffraction (XRD) analysis

Fig. 1 shows the X-ray diffraction spectra for the stoichiometric CTLA powders calcined at various temperatures. Powders calcined at 1150 °C contained $La(OH)_3$ as intermediate phase. The amount of intermediate phase reduced as the calcination temperature was increased to 1250 °C. The powders calcined at 1350 °C were single phase but very hard, making it difficult to reduce them to fine powders. Therefore, 1250 °C was chosen as the calcinations temperature for the CTLA ceramics.

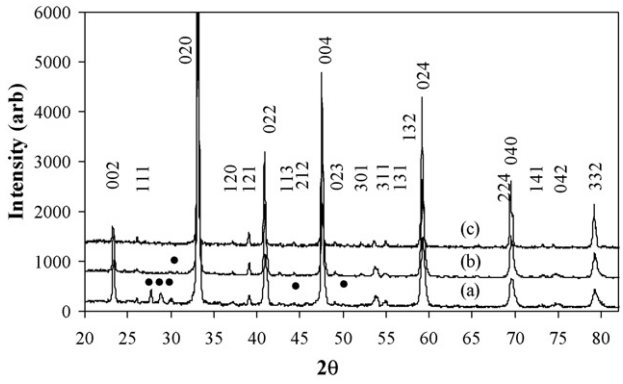

Fig. 1. X-ray diffraction spectra for CTLA powder calcined at: (a) 1150 °C, (b) 1250 °C and (c) 1350 °C, (●) the intermediate phase $La(OH)_3$ identified.

Fig. 2 shows the X-ray diffraction spectrum for CTLA ceramics prepared with different levels of Al_2O_3. The reflections are consistent with that for a tilted perovskite structure. The pattern can be interpreted as an orthorhombic structured perovskite phase containing of both in-phase and anti-phase tilting of BO_6 octahedral in association with anti-parallel shifting of A-site cations. From the reflections, there was no evidence of a secondary phase.

The addition of Al_2O_3 did not change the lattice parameters significantly. Samples doped with 0.25 wt% Al_2O_3 had lattice parameters of $a = 5.4072$ (3) Å, $b = 5.4192$ (4) Å and $c = 7.6467$ (4) Å. The unit cell values obtained are consistent with the results found by Kalyavin et al.[11] since *Pnma* space group assigned in the above refinement doubling of the unit cell with respect to *b*-axis is observed ($a^-b^+a^-$). From this study, it was learnt that the CTLA XRD can be better described with orthorhombic *Pbnm* space group and $a^-a^-c^+$ tilt system, which is consistent with CTNA[12] structure at room temperature.

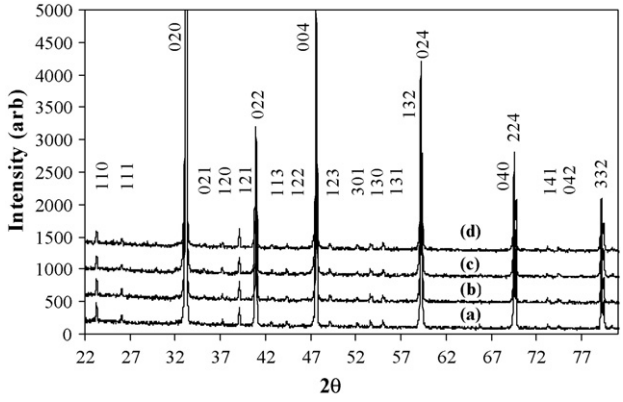

Fig. 2. X-ray diffraction spectra of CTLA prepared with the addition of: (a) 0.15% Al_2O_3, (b) 0.25% Al_2O_3, (c) 0.3% Al_2O_3 and (d) 0.5% Al_2O_3. The samples were sintered at 1500 °C for 4 h and cooled at 180 °C/h.

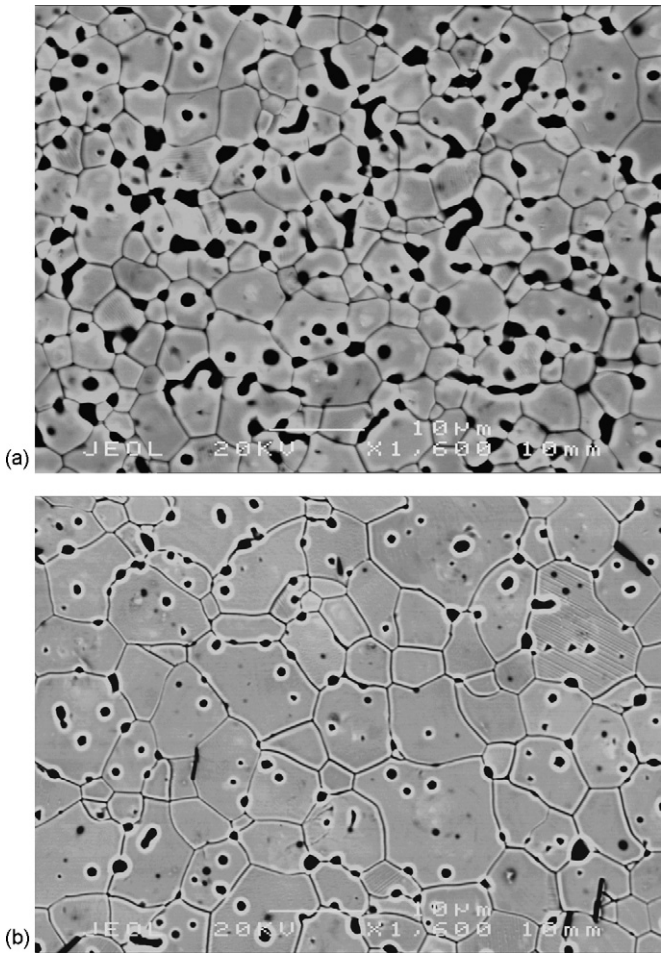

Fig. 3. The back scattered SEM images of CTLA: (a) 0% Al_2O_3 and (b) 0.25% Al_2O_3.

3.3. Microstructure

Fig. 3 shows back scattered SEM images of polished and thermally etched surfaces of CTLA samples sintered at 1500 °C for 4 h. The grain size of CTLA ceramics increased from approximately 5 μm for undoped samples to approximately 10 μm for samples prepared with 0.15 and 0.25 wt% Al_2O_3. Grain size reduced to approx 4 μm when the amount of Al_2O_3 increased to 0.3 and 0.5 wt% Al_2O_3. The excess alumina addition clearly acts as a grain growth inhibitor, possibly by coating individual CTLA grains.

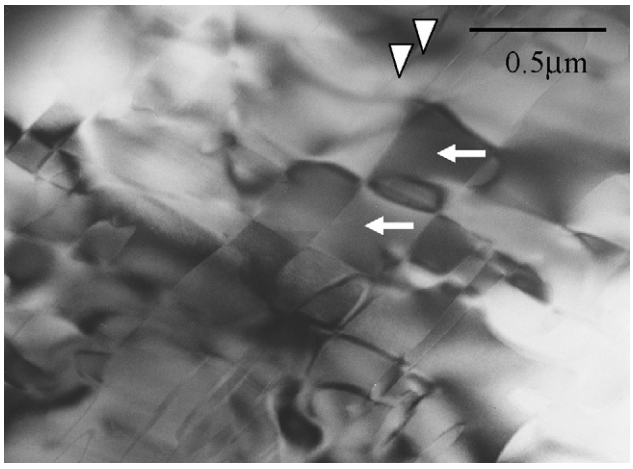

Fig. 4. TEM image of $Ca_{0.7}Ti_{0.7}La_{0.3}Al_{0.3}O_3$ ceramic showing (←) twined domains and (▼) anti-phase boundaries.

Fig. 4 shows a bright field TEM image of CTLA ceramic with 0.25% Al_2O_3 sintered at 1500 °C for 4 h and cooled at 5 °C/h, sub-grain structures can be seen. Selected area diffraction pattern (SAD) studies showed the sub-grain domains have twinned structures; examples are identical in Fig. 4. Anti-phase boundaries resulting from loss of transitional symmetry upon the anti-phase parallel shifting of A-site cations were also observed.

Fig. 5 shows SAD patterns taken from different domains of CTLA with 0.25% Al_2O_3 sintered at 1500 °C for 4 h and cooled at 5 °C/h sample. Fig. 5a is untwined domain viewed along [1 − 1 0] zone axis. Fig. 5b represents [0 0 1] zone of the twined domain after a mirror operation along the plane (−1 1 2). Fig. 5c is the SAD pattern resulting from multiple domains. The (−1 1 2) type twin results from symmetry loss upon cubic to tetragonal transition during cooling from sintering temperature.[3]

Fig. 6 shows SAD patterns taken from different domains of CTLA with 0.25% Al_2O_3 sintered at 1500 °C for 4 h and cooled at 5 °C/h sample. Fig. 6a is untwined domain viewed along the [0 1 0] zone axis. Fig. 6b represents the [1 0 0] zone of the twined domain after a mirror operation along the plane (1 1 0). Fig. 6c is the SAD pattern resulting from multiple domains. The (1 1 0) type twin results from symmetry loss upon tetragonal to orthorhombic transition during cooling from sintering temperature.[3]

In summary, two distinct types of twins on {1 1 2} and {1 1 0} planes were identified in CTLA ceramics. The two twin types

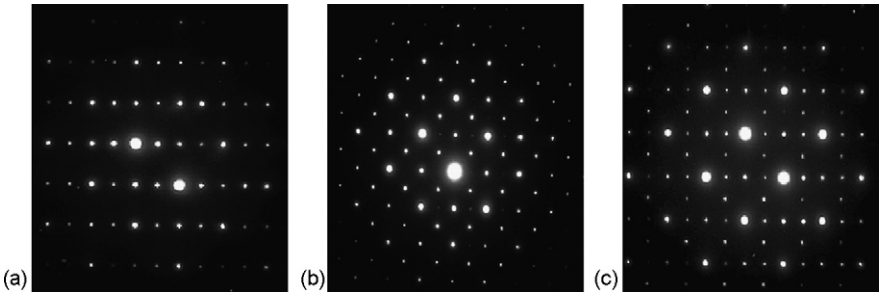

Fig. 5. SAD patterns taken from different domains are shown: (a) [1 − 1 0] zone axis SAD of a single domain, (b) [0 0 1] zone axis SAD of the twinned domain and (c) multi-domain diffraction pattern from a and b.

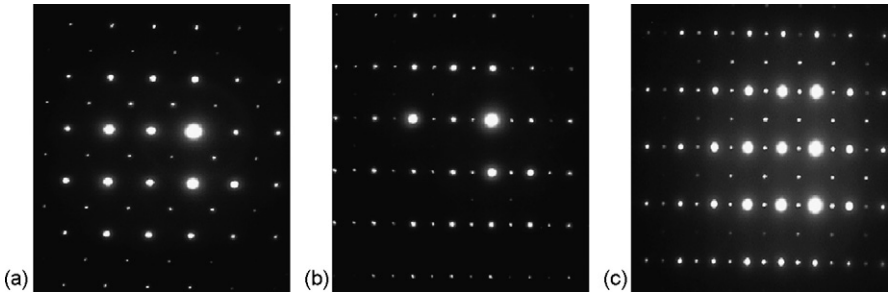

Fig. 6. SAD patterns taken from different domains are shown: (a) [0 1 0] zone axis SAD of a single domain, (b) [1 0 0] zone axis SAD of the twinned domain and (c) multi-domain diffraction pattern from a and b.

have been previously reported to occur in orthorhombic perovskites and are associated with cubic–tetragonal–orthorhombic transitions when the specimens are cooled to room temperature.[3]

A second phase was observed in samples prepared with excess Al_2O_3 (Fig. 7). EDS analysis showed that it is rich in Al and Ca. The grains are typically 2–5 μm long and 0.5 μm wide, needle shaped distributed mainly along grain boundaries. The amount of the second phase was less then 2% of the sample volume, which is why it was not detected in X-ray diffraction analysis. A low melting point eutectic at approximately 1350 °C has been reported to exist in the CaO–Al_2O_3 binary system.[13,14] The formation of this phase is thought to be responsible for the improvement in density.

3.4. Microwave dielectric properties

Microwave dielectric properties of CTLA ceramic were affected by the presence of Al_2O_3 additions. There was a clear increase to maxima in both ε_r and $Q \times f$ as Al_2O_3 level increased to 0.25 wt% (Table 1). The peak in dielectric properties coincides with maximum densification, demonstrating the importance of high density.

For CTLA samples prepared with 0.25 wt% Al_2O_3 the dielectric properties were sensitive to the cooling rate (Fig. 8). As samples were cooled at slower rate, the ceramics spent more time at elevated temperatures, there was a significant improvement in both ε_r and $Q \times f$ values. As the cooling rate reduced from 180 to 5 °C/h, the relative permittivity increase from 43.5 to 46, and $Q \times f$ increase from 35,000 to 38,000 GHz. Both reflect improvements in densification and the microstructure. The temperature coefficient of resonant frequency has typically +12 ppm/°C at 4 GHz for the CTLA ceramics.

Table 1
Microwave dielectric properties of CTLA as a function of Al_2O_3 addition

Weight % Al_2O_3	Dielectric constant (ε_r)	$Q \times f$ (GHz)	Density ratio (%)
0	41.44	26,618	90
0.15	42.32	33,833	93
0.25	43.28	35,157	93
0.30	43.08	34,154	92
0.50	42.36	32,134	90

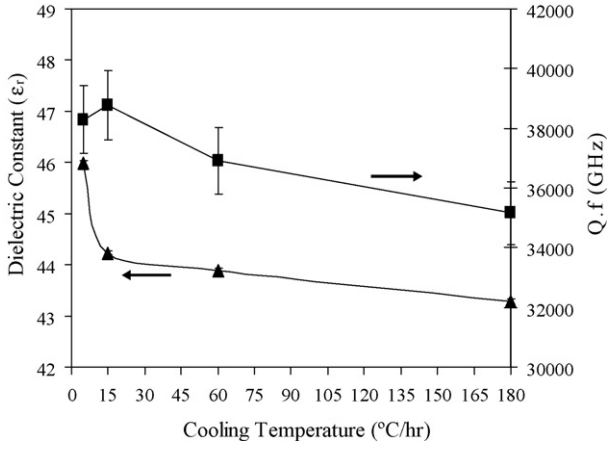

Fig. 8. ε_r and $Q \times f$ values of CTLA + 0.25% Al_2O_3 ceramics as a function of cooling rate.

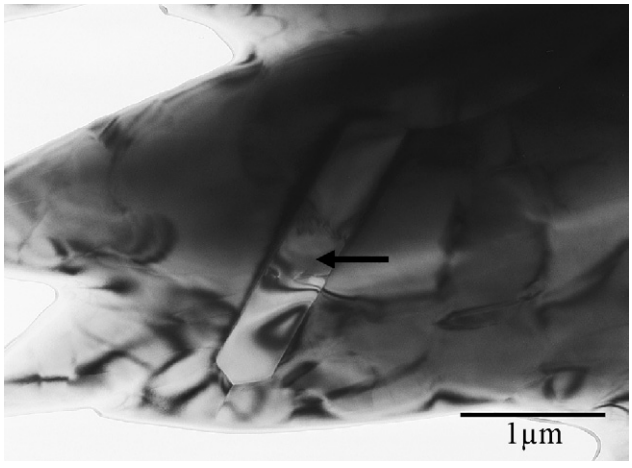

Fig. 7. TEM image of $Ca_{0.7}Ti_{0.7}La_{0.3}Al_{0.3}O_3$ ceramic showing (←) Ca–Al rich second phase.

4. Conclusions

High density CTLA was prepared by Al_2O_3 addition, the samples sintered at 1500 °C with 0.25% Al_2O_3 addition exhibits $\varepsilon_r = 46$, $Q \times f = 38{,}289$ and $\tau_f = +12$ at 4 GHz compared to the undoped $\varepsilon_r = 41$, $Q \times f = 26{,}618$. The second phase CaO–Al_2O_3 was observed with excess Al_2O_3 samples, this phase thought to be responsible for the improvement in the density and dielectric

property. Structural study (XRD and TEM) showed that CTLA ceramics are orthorhombic *Pbnm* structure at room temperature with (1 1 2), (1 1 0) twinnings and APBs, which are associated to the high temperature order to the lower temperature disorder phase transformation.

Acknowledgements

The supply of powders by Filtronic Comtek, and support of the EPSRC through GR/R72655/01 and GR/T19148/01 is gratefully acknowledged.

References

1. Chen, T. Y. and Fung, K. Z., Comparison of dissolution behavior and ionic conduction between Sr and/or Mg doped $LaGaO_3$ and $LaAlO_3$. *J. Power Sources*, 2004, **132**, 1–10.
2. Wang, Y., Guyot, F., Yeganesh-Haeri, A. and Liebermann, R. C., Twinning in $MgSiO_3$ perovskites. *Science*, 1990, **248**, 468–471.
3. Wang, Y. and Liebermann, R. C., Electron microscopy study of domain structure due to phase transitions in natural perovskite. *Phys. Chem. Miner.*, 1993, **20**, 147–158.
4. Jancar, B., Suvorov, D., Valant, M. and Drazic, G., Characterization of $CaTiO_3$–$NdAlO_3$ dielectric ceramics. *J. Eur. Ceram. Soc.*, 2003, **23**, 1391–1400.
5. Sasaki, S., Prewitt, C. T., Bass, J. D. and Schulze, W. A., Orthorhombic perovskite $CaTiO_3$ and $CdTiO_3$: structure and space group. *Acta Cryst.*, 1987, **C43**, 1668–1674.
6. Suvorov, D., Valant, M., Jancar, B. and Skapin, S. D., $CaTiO_3$-based ceramics: microstructural development and dielectric properties. *Acta Chim. Slov.*, 2001, **48**, 87–99.
7. Cho, S. Y., Kim, I. T. and Hong, K. S., Microwave dielectric properties and applications of rare-earth aluminates. *J. Mater. Res.*, 1999, **14**, 114–119.
8. Nenasheva, E. A., Mudroliubova, L. P. and Kartenko, N. F., Microwave dielectric properties of ceramics based on $CaTiO_3$–$LnMO_3$ system (Ln–La, Nd; M–Al, Ga). *J. Eur. Ceram. Soc.*, 2003, **23**, 2443–2448.
9. Moon, J. H., Jang, H. M., Park, H. S., Shin, J. Y. and Kim, H. S., Sintering behaviour and microwave dielectric properties of $(Ca,La)(Ti,Al)O_3$ ceramics. *Jpn. J. Appl. Phys.*, 1999, **38**, 6821–6826.
10. Hakki, B. W. and Coleman, P. D., A dielectric resonator method of measuring inductive capacitance in the millimetre range. *IEEE Trans. Microwave Theory Tech.*, 1980, **MTT-18**, 402–410.
11. Kalyavin, D. D., Salak, A. N., Senos, A. M. R., Mantas, P. Q. and Ferreira, V. M., Structure sequence in the $CaTiO_3$–$LaAlO_3$ microwave ceramics—revised. *J. Am. Ceram. Soc.*, 2006, **89**, 1721–1723.
12. Kipkoech, E. R., Azough, F., Freer, R., Leach, C., Thompson, S. P. and Tang, C. C., Structural study of $Ca_{0.7}Nd_{0.3}Ti_{0.7}Al_{0.3}O_3$ dielectric ceramic using synchrotron X-ray diffraction. *J. Eur. Ceram. Soc.*, 2003, **23**, 2677–2682.
13. Zaitsev, A. I., Korolyev, N. V. and Mogutnov, B. M., *J. Mater. Sci.*, 1991, **26**(6), 1588–1600.
14. Zaitsev, A. I., Korolyev, N. V. and Mogutnov, B. M., *High Temp. Sci.*, 1989, **28**, 351–377.